Electronic Supplementary Material (ESI) for Physical Chemistry Chemical Physics.

Supporting Information

Investigation of electronic and vibrational properties of Dihydroxylammonium 5,5'-bistetrazole-1,1'-diolate under high pressure conditions

Junyu Fan, Yan Su,* and Jijun Zhao

Key Laboratory of Materials Modification by Laser, Ion and Electron Beams (Dalian University of Technology), Ministry of Education, Dalian, 116024, China

* Corresponding author. E-mail: su.yan@dlut.edu.cn

1. Raman spectra at hydrostatic conditions

The Raman characteristics under hydrostatic pressure have been well studied by Dreger and his colleagues.[S1] The results of hydrostatic Raman spectra in this work are consistent with the observation in previous experiments and calculations.[S1]

Detailed comparisons of the selected Raman shift between calculated and experimental results are presented in Figure S4. Pressure dependence of Raman spectra under hydrostatic compressions is shown in Figure 5a. The high-wavenumber modes (v_1−v_4), associated with cation moieties are predicted at 2650−3200 cm^{-1}. The NH_2 asymmetric stretching (v_1) presents a red shift before 3 GPa, then the red shift reverts gradually to a blue shift. This fact manifests the lengthening of N_1−H_2 covalent bond at first and starts to shorten the N_1−H_2 bond due to the compression of space after 3 GPa (see section 3.1 and Figure S5). The red shift is also observed in NH_2 symmetric stretch (v_2) due to the slight lengthening of the N_1−H_1 covalent bonds with increasing pressure. Similarly, the mode mixed NH and OH character (v_4) presents a red shift, while the wavenumber of v_3 mode (NH and OH symmetrical stretching) is gradually increasing under higher pressure. From the vibrational pattern of TKX-50, we noted that the N_1−H_3 bond participates in v_3 vibrational mode with the relatively strong contribution while the O_1−H_4 bond mainly participates in v_4 vibrational mode. Thus, the blue shift of v_3 and red shift of v_4 are associated with the slight shortening of N_1−H_1 and lengthening of O_1−H_4 bonds at 0−10 GPa, respectively.

Examination of Table S2 shows that most vibrational modes of TKX-50 are combinations of both cation and anion vibrations at ambient condition. The Raman frequencies of these modes increase with elevated pressure in most case below 1600 cm^{-1}. The highest coefficient (8.13 cm^{-1} GPa^{-1}) is observed for the low-frequency internal mode v_{29}, while the lattice modes have coefficients less than 2.99 cm^{-1} GPa^{-1}. In our previous work,[S2] the highest coefficient of lattice modes for RDX is up to 9.0 cm^{-1} GPa^{-1}, which indicate TKX-50 may have stronger intermolecular interactions than the typical nitro explosive like RDX.

Table S1. Characteristics of vibrational modes in TKX-50 crystal at ambient pressure. dv/dp is slope of pressure-induced Raman shift. Abbreviation: st: stretch, sci: scissor, bre: breathe, sym: symmetric, asym: asymmetric.

Mode	Wavenumber /cm^{-1}			Assignment		dv/dp /cm^{-1} GPa^{-1}	
	Expt.[S1]	This work	sym.	$(NH_3OH)^+$	$(C_2N_8O_2)^{2-}$	This work	Expt.[S1]
v_1	3216	3186	A_g	NH_2 asym st		−0.70	−2.05
		3197	B_g				
v_2	3170	3120	A_g	NH_2 sym st		−5.96	−0.86
		3132	B_g				
v_3	2931	2897	A_g	NH sym st +		6.94	4.21
		2898	B_g	OH sym st			
v_4		2652	A_g	NH sym st +		−8.09	
		2654	B_g	OH sym st			
v_5	1650	1586	A_g	NH_2 sci		5.02	6.76
		1592	B_g				
v_6	1615	1578	A_g	NH_2 sci		1.69	6.04
		1579	B_g				
v_7	1592	1569	A_g	NH_2 sci	C-C sym st	1.29	5.78
		1567	B_g				
v_8	1590	1550	A_g	NH_2 sci + NH		−2.20	−0.76
		1558	B_g	rock + OH rock			
v_9	1485	1504	A_g	NH_2 sci + NH		−2.19	3.47
		1516	B_g	rock + OH rock			
v_{10}	1467	1425	A_g	NH rock + OH	C-N sym st	4.72	2.03
		1431	B_g	rock			
v_{11}	1276	1250	A_g	NH rock + OH	$(CN_3)_2$ deformation	3.64	3.18
		1257	B_g	rock			
v_{12}	1239	1212	A_g	NH rock + OH		2.58	3.71
		1221	B_g	rock			
v_{13}	1185	1202	A_g	NH rock + OH	$(N_3)_2$ sci	3.42	2.14
		1203	B_g	rock			
v_{14}	1171	1159	A_g	NH rock + OH		−0.94	1.33
		1167	B_g	rock			
v_{15}	1133	1094	A_g		$(N_3)_2$ sci	3.19	2.64
		1095	B_g				
v_{16}	1116	1067	A_g	NH rock + OH	$(N_3)_2$ sci	4.71	3.09
		1067	B_g	rock			
v_{17}	1016	1007	A_g	NO sym st +		4.62	4.75
		1010	B_g	NH_3OH bre			
v_{18}	1006	963	A_g		C-N sym st	2.45	2.17

		965	B_g		+ N-N-N sci		
v_{19}		867	A_g	OH rock		6.39	
		873	B_g				
v_{20}	761	755	A_g	OH wag	Ring	3.75	3.79
		755	B_g		deformation		
v_{21}	742	714	A_g		Ring	0.02	0.29
		714	B_g		deformation + C-C rock		
v_{22}	701	663	A_g		Ring	1.16	1.12
		664	B_g		deformation + C-C rock		
v_{23}	610	598	A_g	OH st	Ring rock	2.14	2.17
		598	B_g				
v_{24}	433	431	A_g	NH_3 rock + OH rock	Ring deformation	4.15	2.71
		427	B_g				
v_{25}	407	404	A_g		Ring	3.17	3.01
		403	B_g		deformation		
v_{26}	333	350	A_g	NH_3 rock		5.78	4.64
		347	B_g				
v_{27}	295	328	A_g	NH_3 rock + OH st		5.61	7.90
		344	B_g				
v_{28}		308	A_g	NH_3 rock + OH st		6.56	
		303	B_g				
v_{29}	256	278	A_g	NH_3 rock + OH st	Ring deformation	8.13	9.76
		262	B_g				
v_{30}	220	229	A_g	NH_3 st		5.58	7.31
		239	B_g				
v_{31}	196	209	A_g	rotation	Ring	4.88	5.42
		215	B_g		deformation		
v_{32}	139	146	A_g	rotation	Ring	7.12	6.78
		168	B_g		deformation		
v_{33}	121	130	A_g	translation	Ring	4.75	7.46
		131	B_g		deformation		
v_{34}	115	113	A_g	rotation	Ring	2.46	7.14
		125	B_g		deformation		
v_{35}	103	103	A_g	translation	Ring	1.17	3.18
		117	B_g		deformation		
v_{36}	58	62	A_g	rotation	rotation	2.99	2.54
		71	B_g				

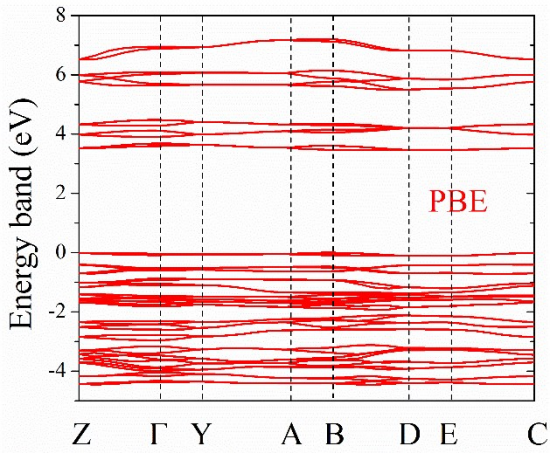

Figure S1. The electronic structure of TKX-50 at ambient condition.

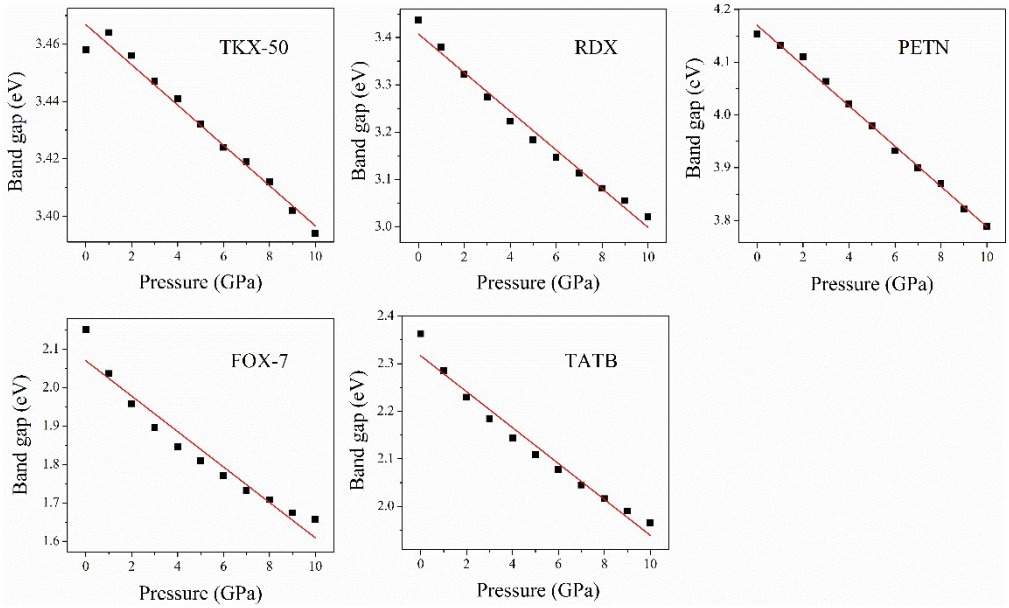

Figure S2. The evolutions of band gap of five energetic materials under hydrostatic pressure. The least-squares fitting is used to examine slop of band gap.

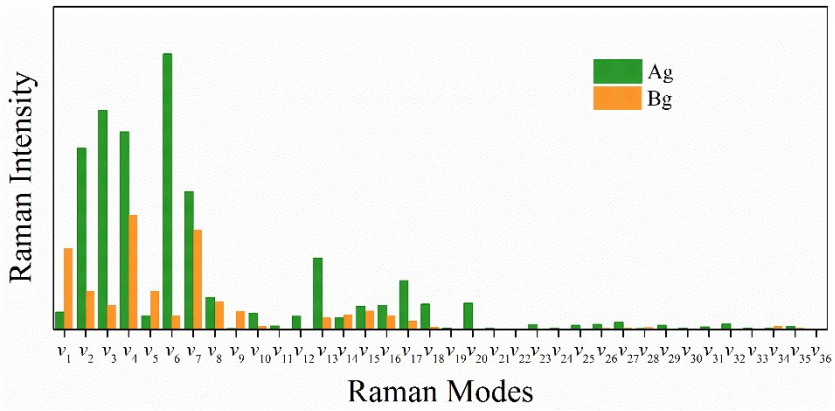

Figure S3. The intensities of A_g and B_g symmetry of modes are compared at 0K.

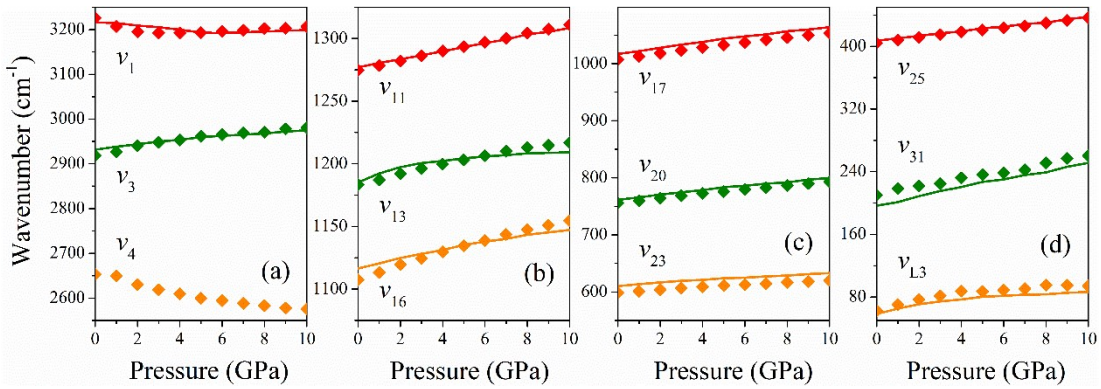

Figure S4. Raman shifts of selected characteristic peaks under pressure. The dots and lines depict the Raman shifts of this work and experiment, respectively. The calculated frequencies at all pressures are shifted by the same amount so that the calculated values and the experimental values match at ambient pressure.

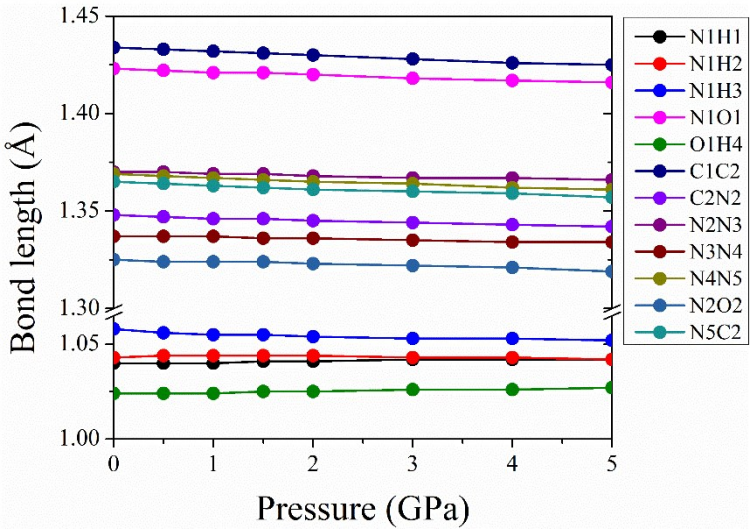

Figure S5. The pressure dependence of molecular bond lengths.

References

S1 Z. A. Dreger, Y. Tao, B. B. Averkiev, Y. M. Gupta and T. M. Klapotke, *J. Phys. Chem. B*, 2015, **119**, 6836-6847.

S2 J. Fan, Y. Su, Z. Zheng, Q. Zhang and J. Zhao, *J. Raman Spectrosc.*, 2019, **50**, 889-898.